

W and Z Boson Production in $p\bar{p}$ Collisions at $\sqrt{s} = 1.8$ TeV

S. Abachi,¹² B. Abbott,³³ M. Abolins,²³ B. S. Acharya,⁴⁰ I. Adam,¹⁰ D. L. Adams,³⁴ M. Adams,¹⁵ S. Ahn,¹² H. Aihara,²⁰ J. Alitti,³⁶ G. Álvarez,¹⁶ G. A. Alves,⁸ E. Amidi,²⁷ N. Amos,²² E. W. Anderson,¹⁷ S. H. Aronson,³ R. Astur,³⁸ R. E. Avery,²⁹ A. Baden,²¹ V. Balamurali,³⁰ J. Balderston,¹⁴ B. Baldin,¹² J. Bantly,⁴ J. F. Bartlett,¹² K. Bazizi,⁷ J. Bendich,²⁰ S. B. Beri,³¹ I. Bertram,³⁴ V. A. Bezzubov,³² P. C. Bhat,¹² V. Bhatnagar,³¹ M. Bhattacharjee,¹¹ A. Bischoff,⁷ N. Biswas,³⁰ G. Blazey,¹² S. Blessing,¹³ P. Bloom,⁵ A. Boehnlein,¹² N. I. Bojko,³² F. Borchering,¹² J. Borders,³⁵ C. Boswell,⁷ A. Brandt,¹² R. Brock,²³ A. Bross,¹² D. Buchholz,²⁹ V. S. Burtovoi,³² J. M. Butler,¹² D. Casey,³⁵ H. Castilla-Valdez,⁹ D. Chakraborty,³⁸ S.-M. Chang,²⁷ S. V. Chekulaev,³² L.-P. Chen,²⁰ W. Chen,³⁸ L. Chevalier,³⁶ S. Chopra,³¹ B. C. Choudhary,⁷ J. H. Christenson,¹² M. Chung,¹⁵ D. Claes,³⁸ A. R. Clark,²⁰ W. G. Cobau,²¹ J. Cochran,⁷ W. E. Cooper,¹² C. Cretsinger,³⁵ D. Cullen-Vidal,⁴ M. A. C. Cummings,¹⁴ D. Cutts,⁴ O. I. Dahl,²⁰ K. De,⁴¹ M. Demarteau,¹² R. Demina,²⁷ K. Denisenko,¹² N. Denisenko,¹² D. Denisov,¹² S. P. Denisov,³² W. Dharmaratna,¹³ H. T. Diehl,¹² M. Diesburg,¹² G. Di Loreto,²³ R. Dixon,¹² P. Draper,⁴¹ J. Drinkard,⁶ Y. Ducros,³⁶ S. R. Dugad,⁴⁰ S. Durston-Johnson,³⁵ D. Edmunds,²³ J. Ellison,⁷ V. D. Elvira,^{12,*} R. Engelmann,³⁸ S. Eno,²¹ G. Eppley,³⁴ P. Ermolov,²⁴ O. V. Eroshin,³² V. N. Evdokimov,³² S. Fahey,²³ T. Fahland,⁴ M. Fatyga,³ M. K. Fatyga,³⁵ J. Featherly,³ S. Feher,³⁸ D. Fein,² T. Ferbel,³⁵ G. Finocchiaro,³⁸ H. E. Fisk,¹² Yu. Fisyak,²⁴ E. Flattum,²³ G. E. Forden,² M. Fortner,²⁸ K. C. Frame,²³ P. Franzini,¹⁰ S. Fuess,¹² A. N. Galjaev,³² E. Gallas,⁴¹ C. S. Gao,^{12,†} S. Gao,^{12,†} T. L. Geld,²³ R. J. Genik II,²³ K. Genser,¹² C. E. Gerber,^{12,‡} B. Gibbard,³ V. Glebov,³⁵ S. Glenn,⁵ B. Gobbi,²⁹ M. Goforth,¹³ A. Goldschmidt,²⁰ B. Gómez,¹ P. I. Goncharov,³² H. Gordon,³ L. T. Goss,⁴² N. Graf,³ P. D. Grannis,³⁸ D. R. Green,¹² J. Green,²⁸ H. Greenlee,¹² G. Griffin,⁶ N. Grossman,¹² P. Grudberg,²⁰ S. Grünendahl,³⁵ W. Gu,^{12,†} J. A. Guida,³⁸ J. M. Guida,³ W. Guryn,³ S. N. Gurzhev,³² Y. E. Gutnikov,³² N. J. Hadley,²¹ H. Haggerty,¹² S. Hagopian,¹³ V. Hagopian,¹³ K. S. Hahn,³⁵ R. E. Hall,⁶ S. Hansen,¹² R. Hatcher,²³ J. M. Hauptman,¹⁷ D. Hedin,²⁸ A. P. Heinson,⁷ U. Heintz,¹² R. Hernández-Montoya,⁹ T. Heuring,¹³ R. Hirosky,¹³ J. D. Hobbs,¹² B. Hoeneisen,^{1,8} J. S. Hoftun,⁴ F. Hsieh,²² Ting Hu,³⁸ Tong Hu,¹⁶ T. Huehn,⁷ S. Igarashi,¹² A. S. Ito,¹² E. James,² J. Jaques,³⁰ S. A. Jerger,²³ J. Z.-Y. Jiang,³⁸ T. Joffe-Minor,²⁹ H. Johari,²⁷ K. Johns,² M. Johnson,¹² H. Johnstad,³⁹ A. Jonckheere,¹² M. Jones,¹⁴ H. Jöstlein,¹² S. Y. Jun,²⁹ C. K. Jung,³⁸ S. Kahn,³ J. S. Kang,¹⁸ R. Kehoe,³⁰ M. L. Kelly,³⁰ A. Kernan,⁷ L. Kerth,²⁰ C. L. Kim,¹⁸ S. K. Kim,³⁷ A. Klatchko,¹³ B. Klima,¹² B. I. Klochkov,³² C. Klopfenstein,³⁸ V. I. Klyukhin,³² V. I. Kochetkov,³² J. M. Kohli,³¹ D. Koltick,³³ A. V. Kostritskiy,³² J. Kotcher,³ J. Kourlas,²⁶ A. V. Kozelov,³² E. A. Kozlovski,³² M. R. Krishnaswamy,⁴⁰ S. Krzywdzinski,¹² S. Kunori,²¹ S. Lami,³⁸ G. Landsberg,¹² R. E. Lanou,⁴ J.-F. Lebrat,³⁶ A. Leflat,²⁴ H. Li,³⁸ J. Li,⁴¹ Y. K. Li,²⁹ Q. Z. Li-Demarteau,¹² J. G. R. Lima,⁸ D. Lincoln,²² S. L. Linn,¹³ J. Linnemann,²³ R. Lipton,¹² Y. C. Liu,²⁹ F. Lobkowicz,³⁵ S. C. Loken,²⁰ S. Lökös,³⁸ L. Lueking,¹² A. L. Lyon,²¹ A. K. A. Maciel,⁸ R. J. Madaras,²⁰ R. Madden,¹³ I. V. Mandrichenko,³² Ph. Mangeot,³⁶ S. Mani,⁵ B. Mansoulié,³⁶ H. S. Mao,^{12,†} S. Margulies,¹⁵ R. Markeloff,²⁸ L. Markosky,² T. Marshall,¹⁶ M. I. Martin,¹² M. Marx,³⁸ B. May,²⁹ A. A. Mayorov,³² R. McCarthy,³⁸ T. McKibben,¹⁵ J. McKinley,²³ H. L. Melanson,¹² J. R. T. de Mello Neto,⁸ K. W. Merritt,¹² H. Miettinen,³⁴ A. Milder,² A. Mincer,²⁶ J. M. de Miranda,⁸ C. S. Mishra,¹² M. Mohammadi-Baarmand,³⁸ N. Mokhov,¹² N. K. Mondal,⁴⁰ H. E. Montgomery,¹² P. Mooney,¹ M. Mudan,²⁶ C. Murphy,¹⁶ C. T. Murphy,¹² F. Nang,⁴ M. Narain,¹² V. S. Narasimham,⁴⁰ A. Narayanan,² H. A. Neal,²² J. P. Negret,¹ E. Neis,²² P. Nemethy,²⁶ D. Nešić,⁴ D. Norman,⁴² L. Oesch,²² V. Oguri,⁸ E. Oltman,²⁰ N. Oshima,¹² D. Owen,²³ P. Padley,³⁴ M. Pang,¹⁷ A. Para,¹² C. H. Park,¹² Y. M. Park,¹⁹ R. Partridge,⁴ N. Parua,⁴⁰ M. Paterno,³⁵ J. Perkins,⁴¹ A. Peryshkin,¹² M. Peters,¹⁴ H. Piekarczyk,¹³ Y. Pischalnikov,³³ A. Pluquet,³⁶ V. M. Podstavkov,³² B. G. Pope,²³ H. B. Prosper,¹³ S. Protopopescu,³ D. Pušeljić,²⁰ J. Qian,²² P. Z. Quintas,¹² R. Raja,¹² S. Rajagopalan,³⁸ O. Ramirez,¹⁵ M. V. S. Rao,⁴⁰ P. A. Rapidis,¹² L. Rasmussen,³⁸ A. L. Read,¹² S. Reucroft,²⁷ M. Rijssenbeek,³⁸ T. Rockwell,²³ N. A. Roe,²⁰ P. Rubinov,³⁸ R. Ruchti,³⁰ S. Rusin,²⁴ J. Rutherford,² A. Santoro,⁸ L. Sawyer,⁴¹ R. D. Schamberger,³⁸ H. Schellman,²⁹ J. Sculli,²⁶ E. Shabalina,²⁴ C. Shaffer,¹³ H. C. Shankar,⁴⁰ R. K. Shivpuri,¹¹ M. Shupe,² J. B. Singh,³¹ V. Sirotenko,²⁸ W. Smart,¹² A. Smith,² R. P. Smith,¹² R. Snihur,²⁹ G. R. Snow,²⁵ S. Snyder,³⁸ J. Solomon,¹⁵ P. M. Sood,³¹ M. Sosebee,⁴¹ M. Souza,⁸ A. L. Spadafora,²⁰ R. W. Stephens,⁴¹ M. L. Stevenson,²⁰ D. Stewart,²² D. A. Stoianova,³² D. Stoker,⁶ K. Streets,²⁶ M. Strovink,²⁰ A. Taketani,¹² P. Tamburello,²¹ J. Tarazi,⁶ M. Tartaglia,¹² T. L. Taylor,²⁹ J. Teiger,³⁶ J. Thompson,²¹ T. G. Trippe,²⁰ P. M. Tuts,¹⁰ N. Varelas,²³ E. W. Varnes,²⁰ P. R. G. Virador,²⁰ D. Vititoe,² A. A. Volkov,³² A. P. Vorobiev,³² H. D. Wahl,¹³ J. Wang,^{12,†} L. Z. Wang,^{12,†} J. Warchol,³⁰ M. Wayne,³⁰ H. Weerts,²³ W. A. Wenzel,²⁰ A. White,⁴¹ J. T. White,⁴² J. A. Wightman,¹⁷ J. Wilcox,²⁷ S. Willis,²⁸ S. J. Wimpenny,⁷

J. V. D. Wirjawan,⁴² J. Womersley,¹² E. Won,³⁵ D. R. Wood,¹² H. Xu,⁴ R. Yamada,¹² P. Yamin,³ C. Yanagisawa,³⁸
 J. Yang,²⁶ T. Yasuda,²⁷ C. Yoshikawa,¹⁴ S. Youssef,¹³ J. Yu,³⁵ Y. Yu,³⁷ Y. Zhang,^{12,†} Y. H. Zhou,^{12,†} Q. Zhu,²⁶
 Y. S. Zhu,^{12,†} Z. H. Zhu,³⁵ D. Zieminska,¹⁶ A. Zieminski,¹⁶ and A. Zylberstejn³⁶

(D0 Collaboration)

¹Universidad de los Andes, Bogotá, Colombia

²University of Arizona, Tucson, Arizona 85721

³Brookhaven National Laboratory, Upton, New York 11973

⁴Brown University, Providence, Rhode Island 02912

⁵University of California, Davis, California 95616

⁶University of California, Irvine, California 92717

⁷University of California, Riverside, California 92521

⁸LAFEX, Centro Brasileiro de Pesquisas Físicas, Rio de Janeiro, Brazil

⁹Centro de Investigación y de Estudios Avanzados, Mexico City, Mexico

¹⁰Columbia University, New York, New York 10027

¹¹Delhi University, Delhi, India 110007

¹²Fermi National Accelerator Laboratory, Batavia, Illinois 60510

¹³Florida State University, Tallahassee, Florida 32306

¹⁴University of Hawaii, Honolulu, Hawaii 96822

¹⁵University of Illinois at Chicago, Chicago, Illinois 60607

¹⁶Indiana University, Bloomington, Indiana 47405

¹⁷Iowa State University, Ames, Iowa 50011

¹⁸Korea University, Seoul, Korea

¹⁹Kyungshung University, Pusan, Korea

²⁰Lawrence Berkeley Laboratory and University of California, Berkeley, California 94720

²¹University of Maryland, College Park, Maryland 20742

²²University of Michigan, Ann Arbor, Michigan 48109

²³Michigan State University, East Lansing, Michigan 48824

²⁴Moscow State University, Moscow, Russia

²⁵University of Nebraska, Lincoln, Nebraska 68588

²⁶New York University, New York, New York 10003

²⁷Northeastern University, Boston, Massachusetts 02115

²⁸Northern Illinois University, DeKalb, Illinois 60115

²⁹Northwestern University, Evanston, Illinois 60208

³⁰University of Notre Dame, Notre Dame, Indiana 46556

³¹University of Panjab, Chandigarh 16-00-14, India

³²Institute for High Energy Physics, 142-284 Protvino, Russia

³³Purdue University, West Lafayette, Indiana 47907

³⁴Rice University, Houston, Texas 77251

³⁵University of Rochester, Rochester, New York 14627

³⁶Commissariat à l'Energie Atomique, DAPNIA/Service de Physique des Particules, CE-Saclay, France

³⁷Seoul National University, Seoul, Korea

³⁸State University of New York, Stony Brook, New York 11794

³⁹SSC Laboratory, Dallas, Texas 75237

⁴⁰Tata Institute of Fundamental Research, Colaba, Bombay 400005, India

⁴¹University of Texas, Arlington, Texas 76019

⁴²Texas A&M University, College Station, Texas 77843

(Received 24 May 1995)

The inclusive cross sections times leptonic branching ratios for W and Z boson production in $p\bar{p}$ collisions at $\sqrt{s} = 1.8$ TeV were measured using the D0 detector at the Fermilab Tevatron collider: $\sigma_W B(W \rightarrow e\nu) = 2.36 \pm 0.07 \pm 0.13$ nb, $\sigma_W B(W \rightarrow \mu\nu) = 2.09 \pm 0.23 \pm 0.11$ nb, $\sigma_Z B(Z \rightarrow e^+e^-) = 0.218 \pm 0.011 \pm 0.012$ nb, and $\sigma_Z B(Z \rightarrow \mu^+\mu^-) = 0.178 \pm 0.030 \pm 0.009$ nb. The first error is the combined statistical and systematic uncertainty, and the second reflects the uncertainty in the luminosity. For the combined electron and muon analyses we find $\sigma_W B(W \rightarrow l\nu)/\sigma_Z B(Z \rightarrow l^+l^-) = 10.90 \pm 0.49$. Assuming standard model couplings, this result is used to determine the width of the W boson, $\Gamma(W) = 2.044 \pm 0.093$ GeV.

PACS numbers: 13.85.Qk, 13.38.-b, 14.70.Fm, 14.70.Hp

The measurement of the production cross sections times leptonic branching ratios (σB) for W and Z bosons allows a determination of the width of the W boson

and a comparison of W and Z boson production with QCD predictions. The total width of the Z boson is known to a precision of 0.3% [1], which places strong

constraints on the existence of new particles produced in neutral weak decays. Our knowledge of the total width of the W boson is an order of magnitude less precise, and the corresponding limits on charged weak decays are much less stringent. It is therefore important to improve the measurement of the W boson width as a means of searching for unexpected W boson decay modes.

We determine the leptonic branching ratio of the W boson, $B(W \rightarrow l\nu)$, from the ratio of the measured W and Z boson σB values

$$R \equiv \frac{\sigma_W B(W \rightarrow l\nu)}{\sigma_Z B(Z \rightarrow ll)}, \quad (1)$$

where $l = e$ or μ , σ_W and σ_Z are the inclusive cross sections for W and Z boson production in $p\bar{p}$ collisions, and $B(Z \rightarrow ll)$ is the leptonic branching ratio of the Z boson. We extract $B(W \rightarrow l\nu)$ from the above ratio using a theoretical calculation of σ_W/σ_Z and the precise measurement of $B(Z \rightarrow ll)$ from LEP. We then combine $B(W \rightarrow l\nu)$ with a theoretical calculation of the W boson leptonic partial width, $\Gamma(W \rightarrow l\nu)$, to obtain the W boson total width, $\Gamma(W)$. Previous measurements of $\Gamma(W)$ have been published by UA1 [2], UA2 [3], and CDF [4,5].

In this Letter, we report a new measurement of σB and determination of $\Gamma(W)$ using data collected with the D0 detector [6] in 1992–93 at the Fermilab Tevatron $p\bar{p}$ collider at $\sqrt{s} = 1.8$ TeV. The four decay channels included in this analysis are $W \rightarrow e\nu, \mu\nu$ and $Z \rightarrow e^+e^-, \mu^+\mu^-$.

Electrons were detected in hermetic, uranium liquid-argon calorimeters [7,8], with an energy resolution of about $15\%/\sqrt{E(\text{GeV})}$. The calorimeters have a transverse granularity of $\Delta\eta \times \Delta\phi = 0.1 \times 0.1$, where η is the pseudorapidity and ϕ is the azimuthal angle.

For the $W \rightarrow e\nu$ and $Z \rightarrow e^+e^-$ analyses we accepted electrons with $|\eta| < 1.1$ or $1.5 < |\eta| < 2.5$. Both the W and Z boson analyses used the same trigger which required a single electron with transverse energy (E_T) greater than 20 GeV. Kinematic selections were made in the off-line analysis requiring that Z boson candidates have two electrons, each with $E_T > 25$ GeV, and that W boson candidates have one electron with $E_T > 25$ GeV and missing transverse energy (\cancel{E}_T) greater than 25 GeV.

The off-line electron identification requirements consisted of three criteria for a “loose” electron: (i) the electron had to deposit at least 95% of its energy in the 21 radiation lengths electromagnetic calorimeter, (ii) the transverse and longitudinal shower shapes had to be consistent with those expected for an electron (based on test beam measurements), and (iii) the electron had to be isolated with $I < 0.1$. The isolation variable is defined as $I = [E_{\text{tot}}(0.4) - E_{\text{EM}}(0.2)]/E_{\text{EM}}(0.2)$, where $E_{\text{tot}}(0.4)$ is the total calorimeter energy inside a cone of radius $\sqrt{\Delta\eta^2 + \Delta\phi^2} = 0.4$ and $E_{\text{EM}}(0.2)$ is the electromagnetic energy inside a cone of 0.2. For a “tight” electron we also required a good match between a reconstructed track in the drift chamber system and the shower position in the calorimeter. For W

boson events we required one “tight” electron, while for Z boson events we required one electron to be tight and the other to be either tight or “loose.” Figures 1(a) and 1(c) show the observed transverse mass and invariant mass distributions for $W \rightarrow e\nu$ and $Z \rightarrow e^+e^-$ candidates passing these cuts. For the $Z \rightarrow e^+e^-$ analysis we used the events in the invariant mass range 75–105 GeV/c^2 .

The kinematic and geometric acceptances (shown in Table I) for the $W \rightarrow e\nu$ and $Z \rightarrow e^+e^-$ channels were calculated with a Monte Carlo simulation using the measured detector resolutions to smear generated four-momenta. The calculation used the CTEQ2M [9] parton distribution functions (PDF), and a NLO calculation [10] of the W boson transverse momentum. The systematic error in the acceptance includes contributions from the uncertainty in the PDF (the spread among CTEQ2 [9], MRS [11], and GRV [12] PDF), from the uncertainty in the W boson mass [13], and from systematic uncertainties associated with modeling the detector response. The trigger and selection efficiencies (Table I) were determined using $Z \rightarrow e^+e^-$ events, where one of the electrons satisfied tight trigger and selection criteria and the second electron provided an unbiased sample to measure the efficiencies. The trigger efficiencies were found to be $>95\%$.

Muons were detected as tracks in three layers of proportional drift tube (PDT) chambers outside the calorimeter. One layer of PDT chambers had four planes and was located inside an iron toroid magnet. The other two layers, each with three planes, were located outside of the iron. The muon momentum resolution in this analysis was $\sigma(1/p) = 0.18(p - 2)/p^2 \oplus 0.008$ (with p in GeV/c). A muon track was required to match a charged track in the central drift chamber system. We accepted muons that passed through the central iron toroid ($|\eta| < 1.0$).

Both the $W \rightarrow \mu\nu$ and $Z \rightarrow \mu^+\mu^-$ analyses used the same trigger, which required a single muon with transverse momentum (p_T) greater than 15 GeV/c . Cosmic ray background was reduced by rejecting muons that also

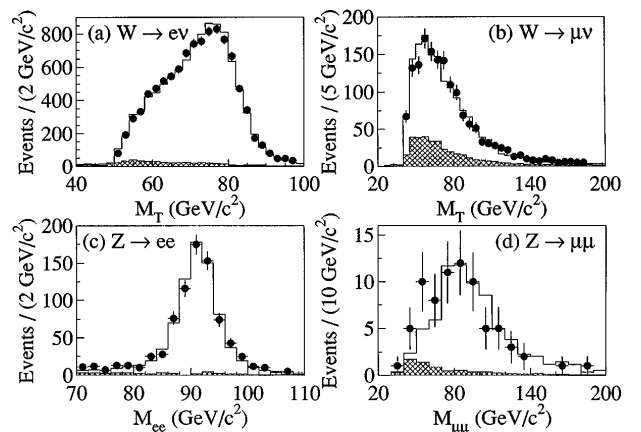


FIG. 1. Transverse mass and invariant mass distributions for the indicated channels. The points are the data. The shaded areas represent the estimated backgrounds, and the solid lines correspond to the sums of the expected signals (from Monte Carlo) and the estimated backgrounds.

TABLE I. Production cross section times leptonic branching ratio for W and Z bosons.

Channel	$W \rightarrow e\nu$	$Z \rightarrow e^+e^-$	$W \rightarrow \mu\nu$	$Z \rightarrow \mu^+\mu^-$
N_{obs}	10338	775	1665	77
Backgrounds(%):				
$Z \rightarrow ee, \mu\mu, \tau\tau$	0.6 ± 0.1	...	7.3 ± 0.5	0.7 ± 0.2
$W \rightarrow \tau\nu$	1.8 ± 0.1	...	5.9 ± 0.5	...
Multijet	3.3 ± 0.5	2.8 ± 1.4	5.1 ± 0.8	2.6 ± 0.8
Cosmic/random	3.8 ± 1.6	5.1 ± 3.6
Drell-Yan	...	1.2 ± 0.1	...	1.7 ± 0.3
Total background(%)	5.7 ± 0.5	4.0 ± 1.4	22.1 ± 1.9	10.1 ± 3.7
Acceptance(%)	46.0 ± 0.6	36.3 ± 0.4	24.8 ± 0.7	6.5 ± 0.4
$\epsilon_{\text{trig}}\epsilon_{\text{sel}}(\%)$	70.4 ± 1.7	73.6 ± 2.4	21.9 ± 2.6	52.7 ± 4.9
$\int \mathcal{L} dt$ (pb $^{-1}$)	12.8 ± 0.7	12.8 ± 0.7	11.4 ± 0.6	11.4 ± 0.6
σB (nb)	2.36	0.218	2.09	0.178
$\pm(\text{stat}), (\text{syst}), (\text{lum})$	$\pm 0.02 \pm 0.07 \pm 0.13$	$\pm 0.008 \pm 0.008 \pm 0.012$	$\pm 0.06 \pm 0.22 \pm 0.11$	$\pm 0.22 \pm 0.021 \pm 0.009$

had hits or tracks within 10° in θ and 20° in ϕ in the muon chambers on the opposite side of the interaction point. Trigger efficiencies were measured using the subsample of events with high p_T muons that satisfied jet or \cancel{E}_T triggers, and also using the second muon in $Z \rightarrow \mu^+\mu^-$ events. The trigger efficiency was about 40% (70%) for W (Z) boson events. Kinematic cuts were made requiring muon $p_T > 20$ GeV/ c and $\cancel{E}_T > 20$ GeV for W boson events, and $p_T > 15, 20$ GeV/ c for the two muons in Z boson events.

A loose muon was required to deposit sufficient energy in the calorimeter to be consistent with the passage of a minimum ionizing particle and to traverse a minimum field integral of 2.0 Tm. This latter requirement restricts the muon analysis to a region of the detector with ≥ 13 interaction lengths of material, so that hadronic punchthrough is negligible. A tight muon had five additional requirements: (i) a stringent track match with a track in the central detector, (ii) a good quality global fit with the vertex and a central detector track, (iii) a muon time of origin within 100 ns of the beam crossing, (iv) energy in the calorimeter consistent with single muon ionization within a cone of radius $\sqrt{\Delta\eta^2 + \Delta\phi^2} = 0.2$ and with less than 6 GeV of additional energy in a cone of 0.6, and (v) a good muon impact parameter.

For Z boson events, we required at least one muon to be tight and the other to be either tight or loose. For W boson events, we required at least one tight muon (after Z boson candidates were removed). Figures 1(b) and 1(d) show the observed transverse mass and invariant mass distributions for $W \rightarrow \mu\nu$ and $Z \rightarrow \mu^+\mu^-$ candidates passing our criteria. The kinematic and geometric acceptances (Table I) were calculated with a full detector Monte Carlo simulation. The selection efficiencies (Table I) were determined with $Z \rightarrow \mu^+\mu^-$ events using the same method that was used for electrons.

The background estimates (Table I) due to $Z \rightarrow e^+e^-$ or $Z \rightarrow \mu^+\mu^-$ (where one of the electrons or muons was lost) and $W \rightarrow \tau\nu$ or $Z \rightarrow \tau^+\tau^-$ (where $\tau \rightarrow e\nu\nu$

or $\mu\nu\nu$) were obtained from Monte Carlo simulations. The multijet background estimate for the $W \rightarrow e\nu$ sample was derived from the data by measuring the tail of the \cancel{E}_T distribution for nonisolated electrons and normalizing this at small \cancel{E}_T to the \cancel{E}_T spectrum for isolated electrons. The multijet background in the $W \rightarrow \mu\nu$ and $Z \rightarrow \mu^+\mu^-$ samples was estimated by comparing the distribution of energy in the calorimeter between the cones of radii of 0.2 and 0.6 around the muons with that measured for events containing a nonisolated muon and jets. The multijet background in the $Z \rightarrow e^+e^-$ sample is due to jet-jet or photon-jet events, where the jets fake an electron in the detector. The amount of this background was estimated by fitting the invariant mass spectrum of the $Z \rightarrow e^+e^-$ events to the sum of the predicted Z boson mass distribution and the experimentally determined multijet background shape. The invariant mass distributions for the jet-jet and photon-jet events were measured separately and then combined to obtain the overall multijet background shape. The cosmic ray and random hit backgrounds to $W \rightarrow \mu\nu$ and $Z \rightarrow \mu^+\mu^-$ were estimated from the distributions of muon time of origin relative to beam crossing.

The luminosity (Table I) was calculated by measuring the rate for $p\bar{p}$ nondiffractive inelastic collisions using two hodoscopes of scintillation counters [6] mounted close to the beam on the front surfaces of the end calorimeters. The normalization for the luminosity measurement and the 5.4% systematic error in the luminosity, which has been estimated from the uncertainty in the $p\bar{p}$ inelastic cross section and uncertainties in the acceptance and efficiency of the counters, are described in Ref. [14].

We calculated σB by subtracting the background from the number of observed events (N_{obs}) and dividing the result by the acceptance, efficiency, and luminosity. The results obtained are shown in Table I and are plotted in Fig. 2, together with the CDF results [15,16] and the theoretical $\mathcal{O}(\alpha_s^2)$ QCD prediction [17,18] of $\sigma_W B(W \rightarrow l\nu) = 2.42^{+0.13}_{-0.11}$ nb and $\sigma_Z B(Z \rightarrow ll) = 0.226^{+0.011}_{-0.009}$ nb.

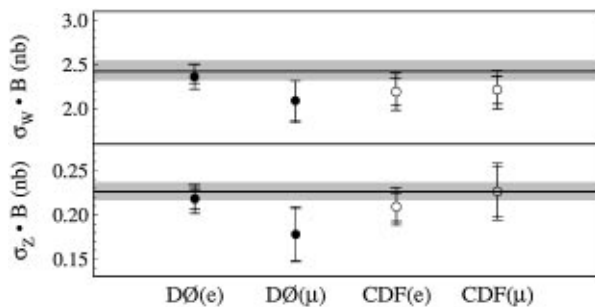


FIG. 2. σB for inclusive W and Z boson production. The inner error bar is the combined statistical and systematic uncertainty and the outer error bar includes the luminosity uncertainty. The solid line and shaded band are the theoretical prediction described in the text.

Using the definition for R in Eq. (1), we obtain for the electron, muon, and combined results

$$R_e = 10.82 \pm 0.41(\text{stat}) \pm 0.30(\text{syst}),$$

$$R_\mu = 11.8_{-1.4}^{+1.8}(\text{stat}) \pm 1.1(\text{syst}),$$

$$R_{e+\mu} = 10.90 \pm 0.49(\text{stat} \oplus \text{syst}).$$

Many common sources of error cancel in R , including the uncertainty in the luminosity and parts of the errors in the acceptance and event selection efficiency.

We use the combined ratio $R_{e+\mu}$ and Eq. (1) to determine $B(W \rightarrow l\nu)$. We use $B(Z \rightarrow ll) = (3.367 \pm 0.006)\%$ [1] and the theoretical calculation [17] of $\sigma_W/\sigma_Z = 3.33 \pm 0.03$, where the quoted error is due to systematic differences in the PDF choices [9,11] (with CTEQ2ML and CTEQ2MS giving the maximum variation) and the uncertainty in the W boson mass [13]. We obtain

$$B(W \rightarrow l\nu) = (11.02 \pm 0.50)\%.$$

We combine this measurement of $B(W \rightarrow l\nu)$ with a theoretical calculation [13,20] of $\Gamma(W \rightarrow l\nu) = 225.2 \pm 1.5$ MeV to obtain

$$\Gamma(W) = 2.044 \pm 0.093 \text{ GeV}.$$

The measurement of $\Gamma(W)$ [or $B(W \rightarrow l\nu)$] can be used to set limits on unexpected decay modes of the W boson, such as W decays into supersymmetric charginos and neutralinos [23], or into heavy quarks [24]. Comparing our result for $\Gamma(W)$ with the standard model prediction, $\Gamma(W) = 2.077 \pm 0.014$ GeV [13,20], the 95% C.L. upper limit on the contribution of unexpected decays to the W boson width is 164 MeV. Combining our result for $\Gamma(W)$ with other measurements [25] gives a weighted average of $\Gamma(W) = 2.062 \pm 0.059$ GeV. Comparing this weighted average with the standard model value gives a 95% C.L. upper limit of 109 MeV on unexpected decays.

We thank the Fermilab Accelerator, Computing, and Research Divisions, and the support staffs at the collabo-

rating institutions for their contributions to the success of this work. We also acknowledge the support of the U.S. Department of Energy, the U.S. National Science Foundation, the Commissariat à l'Énergie Atomique in France, the Ministry for Atomic Energy and the Ministry of Science and Technology Policy in Russia, CNPq in Brazil, the Departments of Atomic Energy and Science and Education in India, Colciencias in Colombia, CONACyT in Mexico, the Ministry of Education, Research Foundation and KOSEF in Korea, and the A. P. Sloan Foundation.

*Visitor from CONICET, Argentina.

†Visitor from IHEP, Beijing, China.

‡Visitor from Universidad de Buenos Aires, Argentina.

§Visitor from Univ. San Francisco de Quito, Ecuador.

- [1] Particle Data Group, L. Montanet *et al.*, Phys. Rev. D **50**, 1173 (1994).
- [2] C. Albajar *et al.*, Phys. Lett. B **253**, 503 (1991).
- [3] J. Alitti *et al.*, Phys. Lett. B **276**, 365 (1992).
- [4] F. Abe *et al.*, Phys. Rev. Lett. **73**, 220 (1994).
- [5] F. Abe *et al.*, Phys. Rev. Lett. **74**, 341 (1995).
- [6] S. Abachi *et al.*, Nucl. Instrum. Methods Phys. Res., Sect. A **338**, 185 (1994).
- [7] H. Aihara *et al.*, Nucl. Instrum. Methods Phys. Res., Sect. A **325**, 393 (1993).
- [8] S. Abachi *et al.*, Nucl. Instrum. Methods Phys. Res., Sect. A **324**, 53 (1993).
- [9] H. L. Lai *et al.*, Phys. Rev. D **51**, 4763 (1995).
- [10] P. B. Arnold and R. P. Kauffman, Nucl. Phys. **B349**, 381 (1991).
- [11] A. D. Martin, R. G. Roberts, and W. J. Stirling, Phys. Lett. B **306**, 145 (1993); **309**, 492(E) (1993).
- [12] M. Glück, E. Reya, and A. Vogt, Z. Phys. C **53**, 127 (1992).
- [13] We used $M_W = 80.23 \pm 0.18$ GeV/ c^2 from D0 Note 2115/CDF Note 2552, 1994 (unpublished).
- [14] J. Bantly *et al.*, Report No. FERMILAB-TM-1930, 1995 (unpublished).
- [15] F. Abe *et al.*, Phys. Rev. D **44**, 29 (1991).
- [16] F. Abe *et al.*, Phys. Rev. Lett. **69**, 28 (1992).
- [17] We calculated $\sigma_W = 22.35$ nb and $\sigma_Z = 6.708$ nb with Ref. [19], using the CTEQ2M PDF [9], $M_Z = 91.19$ GeV/ c^2 [1], M_W from Ref. [13], and $\sin^2 \theta_W \equiv 1 - (M_W/M_Z)^2 = 0.2259$.
- [18] To obtain the predicted σB we used σ from Ref. [17], $B(W \rightarrow l\nu) = (10.84 \pm 0.02)\%$ [20], and $B(Z \rightarrow ll) = (3.367 \pm 0.006)\%$ [1]. The errors in σB include a (2.5–4.5)% error due to the effect of using various PDF choices [9,11] (with CTEQ2ML and CTEQ2MS giving the maximum variation), a 3% error due to using NLO PDF instead of NNLO [21], a (0.2–0.6)% error due to the uncertainty in M_W [13], and a (0.3–0.5)% error due to the variation of the renormalization and factorization scales [22].
- [19] R. Hamberg, W. L. van Neerven, and T. Matsuura, Nucl. Phys. **B359**, 343 (1991).
- [20] J. L. Rosner, M. P. Worah, and T. Takeuchi, Phys. Rev. D **49**, 1363 (1994).
- [21] W. L. van Neerven and E. B. Zijlstra, Nucl. Phys. **B382**, 11 (1992).

-
- [22] A. D. Martin, W. J. Stirling, and R. G. Roberts, *Phys. Rev. D* **50**, 6734 (1994).
- [23] V. Barger *et al.*, *Phys. Rev. D* **28**, 2912 (1983); M. Drees, C. S. Kim, and X. Tata, *Phys. Rev. D* **37**, 784 (1988).
- [24] T. Alvarez, A. Leites, and J. Terrón, *Nucl. Phys.* **B301**, 1 (1988).
- [25] We recalculated $\Gamma(W)$ for the other experiments [2–4] by using their published R values along with the values of $B(Z \rightarrow ll)$ and $\Gamma(W \rightarrow l\nu)$ in this paper. For σ_W/σ_Z we used our value for CDF, and 3.26 ± 0.09 [3] for the UA1 and UA2 experiments at the lower \sqrt{s} .